PAPER

Bioinspired Propulsion Mechanisms Based on Manta Ray Locomotion

AUTHORS

Keith W. Moored
Peter A. Dewey
Mechanical and Aerospace Engineering, Princeton University

Megan C. Leftwich
Physics Division, Los Alamos National Laboratory

Hilary Bart-Smith
Mechanical and Aerospace Engineering, University of Virginia

Alexander J. Smits
Mechanical and Aerospace Engineering, Princeton University

ABSTRACT

Mobuliform swimmers are inspiring novel approaches to the design of underwater vehicles. These swimmers, exemplified by manta rays, present a model for new classes of efficient, highly maneuverable, autonomous undersea vehicles. To improve our understanding of the unsteady propulsion mechanisms used by these swimmers, we report detailed studies of the performance of robotic swimmers that mimic aspects of the animal propulsive mechanisms. We highlight the importance of the undulatory aspect of producing efficient manta ray propulsion and show that there is a strong interaction between the propulsive performance and the flexibility of the actuating surfaces.

Keywords: mobuliform, manta ray, unsteady, swimming, flexible actuators

Introduction

In recent years, there has been considerable interest in developing novel underwater vehicles that use propulsion systems inspired by biology (Colgate & Lynch, 2004; Bandyopadhyay, 2005). Such vehicles have the potential to open up new mission capabilities and improve maneuverability, efficiency, and speed (Fish et al., 2003, 2011). Here we explore how various aspects of biological locomotion relate to performance in the particular case of ray-like swimming, with the aim of informing the design of new vehicles.

The kinematic motion of batoid fish (rays) is based on the chordwise traveling wave that is a hallmark of their motion (Rosenberger, 2001). Species are classified as being oscillatory if the traveling wave wavelength is longer than the chord of their fin and undulatory if the wavelength is less than the chord of their fin. The manta ray is an example of an oscillatory swimmer. Previously, Clark and Smits (2006) explored the thrust production and efficiencies of an artificial pectoral fin that captured the traveling wave motion and observed efficiencies upwards of 50% for an oscillatory motion at a fixed flow velocity.

To study the swimming of mantas, we use artificial or robotic devices that generate a simple baseline motion that approximates biological kinematics. The complexity of the motion is then progressively increased by adding more kinematic features until the motion resembles the biology very closely. At each level of complexity, various performance metrics are measured. We explore the role of spanwise curvature, the effects of a spanwise traveling wave and tip speed modulation, which have not been previously investigated, and, the role of a chordwise traveling wave motion is investigated in the performance of an actively and passively flexible fin.

Experiments

Two biorobotic devices were developed and tested. First, an artificial pectoral fin able to produce root-fixed pure heaving motions was developed and will be referred to as the *heaving fin*. The fin was cast from a flexible plastic and actuated with variable degrees of spanwise curvature. The measurements on the heaving fin were conducted in a tow tank (Figure 1). This facility tows a fin through still water at a *fixed velocity*, U, in a tank measuring 5-m long, 1-m deep, and 1.5-m wide, and we directly measure the net force produced, T, and the power imparted into the fluid, P_f, by a flapping fin structure. The propulsive efficiency of the motion, $\eta_p = \bar{T}U/\bar{P}_f$, can then be calculated from the thrust and power measurements averaged over a cycle, $\bar{T}$ and $\bar{P}_f$, respectively. If the fin were unconstrained and free-swimming, then the net force would cause the fin to accelerate or decelerate to a new velocity where there is no average net force. Constraining the fin allows for the measurement of force production and is a commonly used experimental approach (Anderson et al., 1998).

FIGURE 1

Tow tank facility consisting of an artificial pectoral fin, tow tank, motor, carriage, and a control and measurement system.

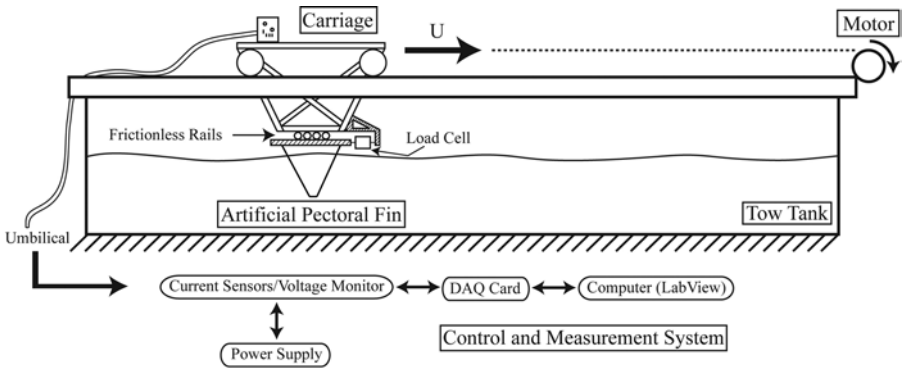

Second, an artificial pectoral fin capable of generating a chordwise traveling wave motion was developed and will be referred to as the *traveling wave fin*. This fin was used to measure the *free-swimming* performance in a tank measuring 6.7-m long, 1-m deep, and 1-m wide. This fin was also cast from a flexible plastic, but it was activated using a number of rigid spars in the spanwise direction. By reducing the number of actuating spars, the degree of passive flexibility of the fin could be varied. The traveling wave wavelength was controlled by changing the phase differences between adjacent spars. The steady swimming speed U and mean power input over a cycle $\bar{P}_f$ were measured, and hence, the energy economy ζ could be found, where $\zeta = U/\bar{P}_f$.

Energy economy is the inverse of cost of transport, both of which are used extensively in the biological literature (Schmidt-Nielsen, 1972; Fish et al., 1991; Liao et al., 2003; Liao, 2004). Energy economy, however, is a more appropriate engineering metric as the dimensions are distance/per unit energy (the units could be miles per gallon for instance). Efficiency is also an appropriate performance measure, but from an experimental point-of-view it can only be measured when there is net thrust production or the fin is not in a free-swimming mode. Thus, for the experiments in the tow tank, efficiency was a measurable performance metric, but in the free-swimming cases, economy is used instead because the efficiency could not be directly measured.

The performance is measured as a function of the Strouhal number, $St = fA/U$, where f is the frequency of motion, A is the peak-to-peak trailing-edge amplitude of motion at the mid-span, and U is the free-stream velocity. The Strouhal number is a measure of the lateral to streamwise spacing of the shed vortices in the wake and to a large extent governs the structure of the wake. It has been shown to be a critical parameter in describing the efficient propulsion of oscillating foils and plates (Anderson et al., 1998; Buchholz & Smits, 2008) and for swimming (Clark & Smits, 2006; Borazjani & Sotiropoulos, 2008, 2009) and flying animals (Taylor et al., 2003).

Fixed Velocity Experiments: Heaving Motion

The skeletal structure of the heaving fin is composed of three connected hinged plates. The angular position of each hinge is individually controlled by a linear actuator. The fin allows for out-of-plane motion with no pitching or undulation in the chordwise direction. The skeletal structure is embedded into a compliant PVC polymer. The PVC is molded around the structure into a fin with a trapezoidal planform shape. This shape was chosen to be a simple representative shape of the manta ray as well as to maximize spacing for the internal structure. The fin has a span length of b = 28 cm and an average chord length of $\overline{c}$ = 19 cm, with an aspect ratio, $AR = b^2/S$, of 1.47, wherein S is the planform area. The cross-sectional shape is a NACA 0020 airfoil. The trailing edge is stiffened by a thin metal sheet attached to the main structure.

Three flapping mode shapes were explored: flat root-fixed heave (Figure 2(a)), curved root-fixed heave (Figure 2(b)), and curved root-fixed heave with a span-wise traveling wave (Figure 2(c)). For each of these mode shapes the tip speed of the fin can be modulated. Previous kinematics studies of ray locomotion (Heine, 1992; Rosenberger, 2001) found that in order to swim faster oscillatory rays do not vary their beat frequency, but instead they vary the tip speed of their fin while holding frequency and amplitude constant. This can be viewed as modifying the actuation waveform to suit a particular mode of swimming. To implement this mode in our experiments, the time-varying waveform was varied from a pure sinusoid towards an almost square wave form (Figure 3). This allows the frequency and amplitude to be held fixed while the maximum fin tip speed is increased. The thrust and propulsive efficiency were measured for each prescribed motion.

FIGURE 2

Swimming modes ranging from an artificial/simple motion that approximates manta ray locomotion to a more complex biologically inspired motion: (a) flat root-fixed heaving motion, (b) curved root-fixed heaving motion, and (c) curved root-fixed heaving motion with a span-wise traveling wave (tip lag effect).

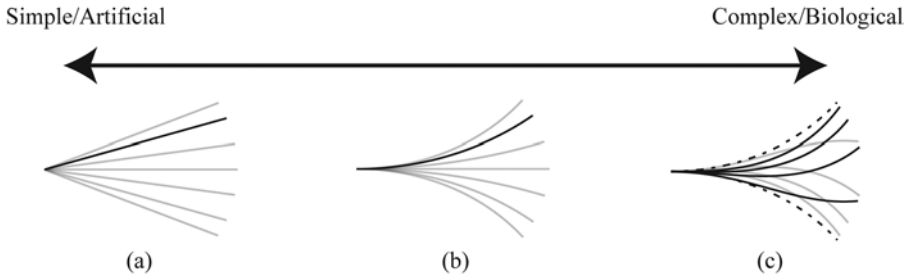

Free-Swimming Experiments: Traveling Wave Motion

The traveling wave fin was tested under free-swimming conditions in a stationary tank to explore the role of flexibility in ray-like propulsion. Low-friction carts were attached to the fin actuation mechanism to form a carriage that was mounted on tracks above the tank (see Figure 4). The chord of the fin was aligned parallel to the tracks, which allowed for a single degree of freedom and made the swimming direction of the carriage unidimensional, and no transverse motion of the carriage was permitted. The root of the fin abutted against an acrylic sheet that was in contact with the free surface of the water to minimize surface waves. Upon actuating the fin, the cart propelled itself down the length of the tank.

An elliptical planform fin with an aspect ratio of 1.6 and a NACA 0020 cross-section was cast using a flexible PVC plastic. Four aluminum spars were embedded into the fin to provide actuation. A push-rod connected each spar to a gear in a gear-train, driven by a DC motor, that produced a sinusoidal rotation of the spar about a pivot point located at the root chord of the fin. This results in a linearly increasing amplitude of motion along the span of the fin (Figure 5). The wavelength of the traveling wave λ could be varied by changing the phase difference between the actuating spars.

In addition, the number of actuating spars could be varied to allow for a certain degree of passive flexibility in the fin. When four actuating spars are used, the locomotion of the fin was prescribed for the entire chord of the fin, with a traveling wave wavelength λ_a, and this fin will be referred to as the active fin. When the two trailing edge spars are removed, the trailing half of the chord of the fin will passively respond to the leading edge actuation and external fluid forces. This fin will be referred to as the passive fin (Figure 5). For the passive fin, the traveling wave along the chord is generated by the first two gears in the gear train and the passive response of the trailing edge. Due to these compounding factors, the precise wavelength along the chord for the passive fin is unknown, and we define an analogous wavelength, λ_p such that $\lambda_a = \lambda_p$ when the offset between the first two gears is identical for both the active and passive fin. We define the dimensionless wavelengths $\lambda_a^* = \lambda_a/C$ and $\lambda_p^* = \lambda_p/C$, where C is the root chord of the fin. This study focuses on cases with $\lambda_a^*, \lambda_p^* > 1$, representative of oscillatory swimmers (Rosenberger, 2001).

FIGURE 3

Holding frequency and amplitude constant while modulating tip speed can be achieved by varying the actuation waveform from a sine wave to a square wave.

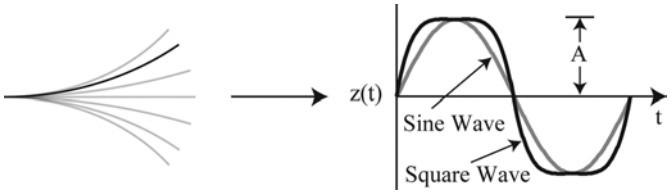

Results and Discussion

Flat and Curved Modes

The first two modes of swimming, the flat mode (Figure 2(a)) and the curved mode (Figure 2(b)), were studied using the heaving fin. The thrust coefficient is defined by $C_T = T/\frac{1}{2}\rho U^2 S$, wherein T is the thrust, ρ is the water density, and S is the planform area of the fin. Similarly, the power coefficient is defined by $C_p = P/\frac{1}{2}\rho U^3 S$, wherein P is the power input to the water (as defined by Clark & Smits, 2006). Figure 6(a) shows that the thrust production and power input increases as the Strouhal number increases, as found in previous studies by Anderson et al. (1998) and Dong et al. (2006). The flat mode of swimming produces more thrust and

FIGURE 4

Tank facility for the chordwise traveling wave experiments: (a) perspective view and (b) front view. Drawings not to scale.

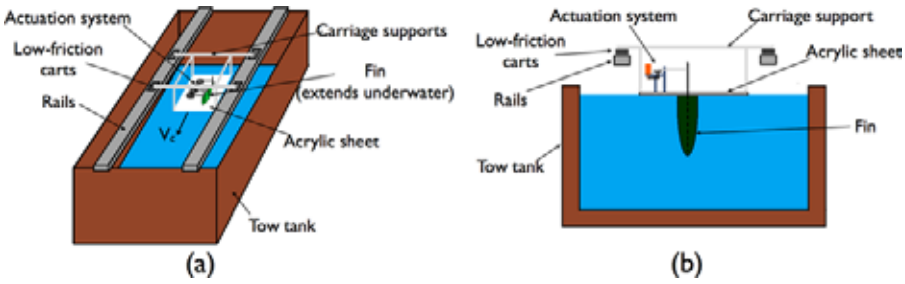

FIGURE 5

Traveling wave actuation system for (left) active fin and (right) passive fin.

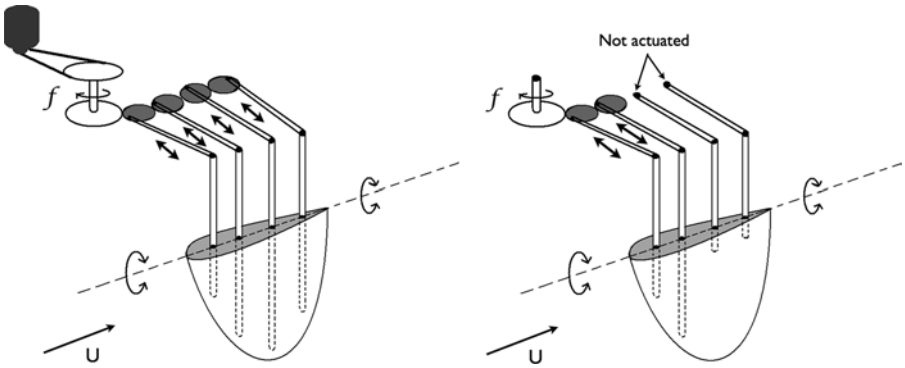

FIGURE 6

Flat mode compared to curved mode: (a) thrust performance as a function of *St* and (b) power coefficient as a function of *St*.

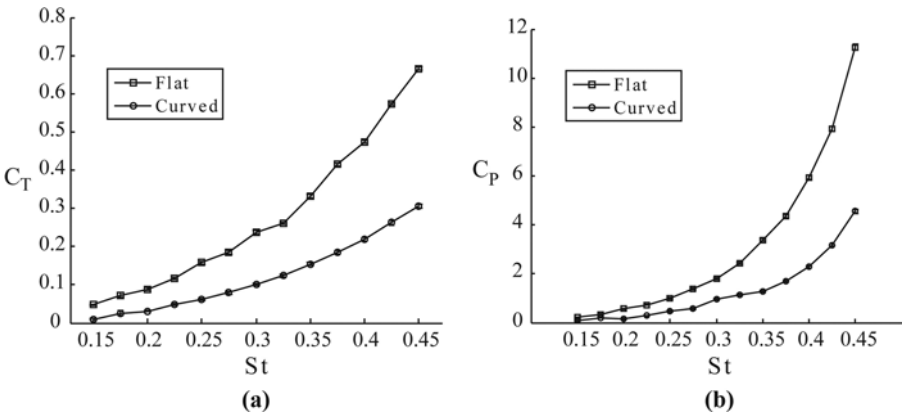

uses more power than the curved mode throughout the Strouhal range. This results is not unexpected as the flat mode of swimming sweeps out a larger volume of fluid than the curved mode of swimming, causing the overall increase in the thrust and power coefficients.

Because the two modes of swimming are dissimilar, comparing the thrust or efficiency as a function of Strouhal number may be misleading. For a fixed Strouhal number, different amounts of thrust and power are produced by each swimming mode. A better comparison is the thrust or efficiency as a function of the power coefficient because each swimming mode can be compared at a fixed power input.

Figure 7a shows this comparison. For both modes of swimming the power input increases as the thrust increases, although at higher power input the thrust increases at a slower rate. For all power inputs, more thrust is produced for the flat mode of swimming than for the curved mode of swimming, while the thrust tends to the drag of the motionless fin as the power input tends to zero. Interestingly, observations of swimming manta rays do not indicate that they use this higher-performance flat mode and instead use the curved mode for swimming. This suggests that the curved mode, coupled with another mechanism (perhaps a chordwise traveling wave), more fully characterizes the swimming mechanics of manta rays.

Figure 7(b) shows the propulsive efficiency as a function of Strouhal number. The efficiency of the curved mode first rises quickly rise with increasing Strouhal number, and then a peak in efficiency is attained, followed by a slow decline in efficiency

FIGURE 7

Flat mode compared to curved mode: (a) thrust coefficient as a function of the power coefficient and (b) efficiency as a function of Strouhal number.

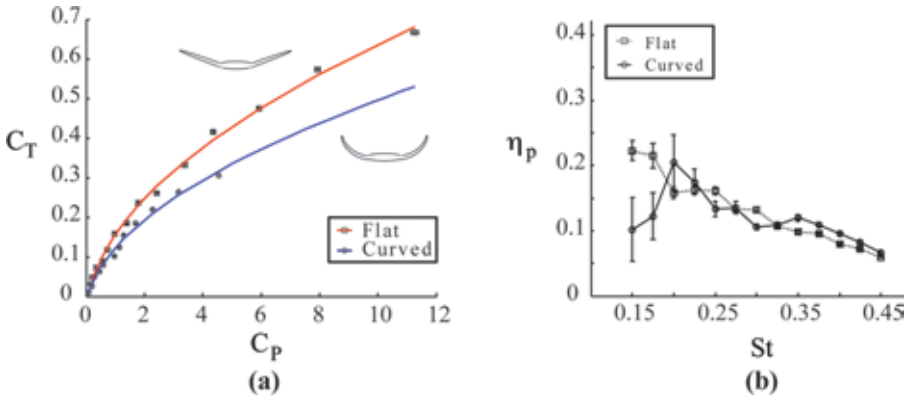

at the higher Strouhal numbers. This trend is characteristic of efficiency curves for oscillating foils and plates (Clark & Smits, 2006; Anderson et al., 1998; Heathcote et al., 2006a, 2006b; Heathcote & Gursul, 2007; Buchholz & Smits, 2008). In general, the efficiency crosses from negative (net drag) to positive (net thrust) and continues to increase while at high values of *St* there is a decline in efficiency that follows potential flow theory (Jones et al., 1998). Thus, a peak in efficiency is expected at an intermediate Strouhal number. The peak efficiency for the curved mode is about 20% occurring at a $St = 0.2$, which is in the range of $0.2 < St < 0.4$ where most swimming and flying species cruise (Taylor et al., 2003). Furthermore, unpublished work on manta rays swimming at different speeds show that a ray swimming at approximately 2 m/s has a Strouhal number of about 0.21 (Fish, 2010), which is in good agreement with our observed value of 0.2 for the peak efficiency of the curved mode. The peak in efficiency for the flat mode is not captured in our experiments, but the highest value seen is about 22%.

Tip Lag Mode

We now study the effects of tip lag for the heaving fin undergoing the curved mode of swimming. Tip lag has been observed as an important feature of manta ray kinematics (Klausewitz, 1964), and here we compare three tip lags: 0, 3.2%, and 11.3%, where the degree of tip lag is the tip deflection normalized by the span as the fin root section crosses the neutral plane (Figure 8). With no tip lag, the entire span crosses the neutral plane at the same time.

The results shown in Figure 9(a) indicate that tip lag increases the thrust and the power coefficients, and the peak in efficiency broadens somewhat for 11.3% tip lag. However, the peak efficiency appears to decrease slightly with increasing tip lag (Figure 9(b)), although the trend is barely outside the uncertainty limits. Perhaps manta rays utilize this kinematic mode to gain a slight thrust increase with no loss of efficiency. However, the artificial fin shape did not capture the sweep that is exhibit by manta rays, as it was thought to be unimportant for thrust production. The sweep could directly affect the streamwise velocity field when tip lag is present and thus more directly affect the thrust and efficiency. In fact, cownose and bullnose rays do not have significant sweep and do not display any significant tip lag (Heine, 1992; Rosenberger, 2001). Furthermore, if a chordwise undulation were present than tip lag would have a greater impact on the streamwise velocity field even when the planform has no sweep.

Tip Speed Modulation

As indicated earlier, myliobatoid rays have been shown to regulate the tip speed of their fins (while holding frequency constant) to increase their swimming speed. To explore this experimentally, the actuation waveform was modified from a sine wave of a given frequency and amplitude towards a square wave with the same frequency and amplitude, but with an increased maximum tip speed (Figure 3). A quartic

FIGURE 8

Diagram showing tip lag effect. The magnitude of tip lag is measured as the tip deflection normalized by the span as the fin root section crosses the neutral plane.

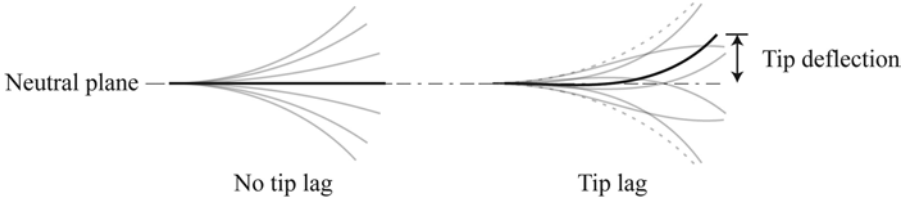

FIGURE 9

Tip lag mode: (a) efficiency as a function of St and (b) peak efficiency dependence on tip lag.

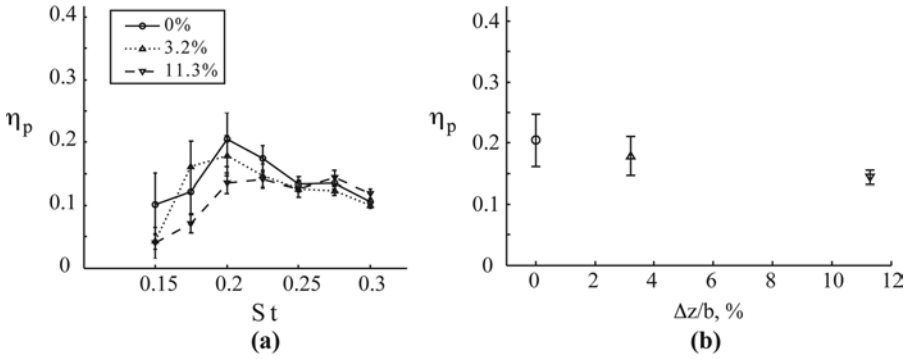

function was used to modulate the tip speed while fixing the frequency and amplitude, as given by

$$x(t) = a(t-\varphi)^4 + b(t-\varphi)^2 + A, \quad 0 \le t \le T/2$$

$$a = \frac{-U_{max}^{sqr}}{2\varphi^3} + \frac{A}{\varphi^4}, b = \frac{-2A}{\varphi^2} + \frac{U_{max}^{sqr}}{2\varphi}$$

$$\varphi = 1/4f, U_{max}^{sqr} = 2\pi\alpha U_\infty St \quad (1)$$

The amplitude, A, the frequency, f, and the maximum tip speed, U_{max}^{sqr}, all determine the shape of the quartic function. The period is T. By holding the frequency and amplitude constant the tip speed can be modulated by varying α between 1 and 2.667. When α is 1, the quartic function matches a sine wave, but when α is 2.667, the maximum tip speed is 2.667 times faster than the maximum tip speed of a sine wave without varying the frequency or amplitude. It should be noted, however, that many animals increase their swimming speed by modulating their frequency of motion while fixing the amplitude. Frequency modulation will increase the Strouhal number by increasing frequency.

Tests were conducted at two Strouhal numbers, 0.2 and 0.25, and the amplitude was fixed at A/b = 0.44 for α =1-2.4. Figure 10a shows the thrust coefficient dependence on the tip speed, α, for a Strouhal number of 0.2. As the tip speed is increased the thrust coefficient increases linearly, indicating that tip speed modulation can be used to increase thrust production, as exhibited by rays (Heine, 1992; Rosenberger, 2001).

Figure 10(b) shows the thrust coefficient plotted against the power coefficient for both frequency modulation and tip speed modulation. Tip speed modulation produces less thrust than frequency modulation for the same input power, suggesting that tip speed modulation is not an efficiency strategy. However, incorporating a chordwise traveling wave may change this outcome. Additionally, as the value of α is increased, the fin has an increasing period of effectively no motion. In a free-swimming test, the increasing resting time for the fin would result in an unpowered gliding period over part of the flapping cycle. This would result in a burst-and-coast behavior that could improve the economy since forward motion would occur without any input power for part of the flapping cycle. Alternatively, tip speed modulation could an effective flight/sprinting mode, where efficiency is not important.

Chordwise Traveling Wave

We now investigate the effects of a chordwise traveling wave, using the traveling wave fin (the experimental arrangement was described in Free-Swimming Experiments: Traveling Wave Motion).

Clark and Smits (2006) investigated the thrust and efficiency of an artificial pectoral fin using a chordwise traveling wave motion and found efficiencies peaking near 50% for optimal conditions ($St \approx 0.25$ and $\lambda_a^* \approx 4$–6). The efficiencies were measured at predetermined Strouhal numbers. For the current work, this constraint is not imposed, and the fin was instead actuated at a given frequency and wavelength and allowed to freely swim down the length of a tow tank. In doing so, the fin attains its self-propelled swimming speed and Strouhal number for that frequency and wavelength.

Figure 11 shows the steady velocity achieved as a function of input flapping frequency for different wavelengths of actuation. The velocity is given in root-chord lengths (CL) per second, where C_{root} = 0.254 m. For the active fin, an almost linear increase in velocity is observed with increasing frequency, a result in agreement with previous studies that found thrust coefficients increasing with frequency (Anderson et al., 1998). Peak velocities were found to occur for $\lambda_a^* = 6$ at the highest flapping frequencies. In these instances the velocity was upwards of 2 CL/s, corresponding to a dimensional velocity of 0.51 m/s, highlighting that this form of propulsion may prove fruitful for future underwater vehicle designs that demand relatively high speeds.

FIGURE 10

(a) Thrust coefficient increasing with tip speed increase and (b) tip speed modulation compared to frequency modulation. The parameter α is the ratio of maximum tip speed of the square wave actuation compared to the maximum tip speed of a sine wave of the same frequency and amplitude, $\alpha = U_{max}^{sqr}/U_{max}^{sin}$.

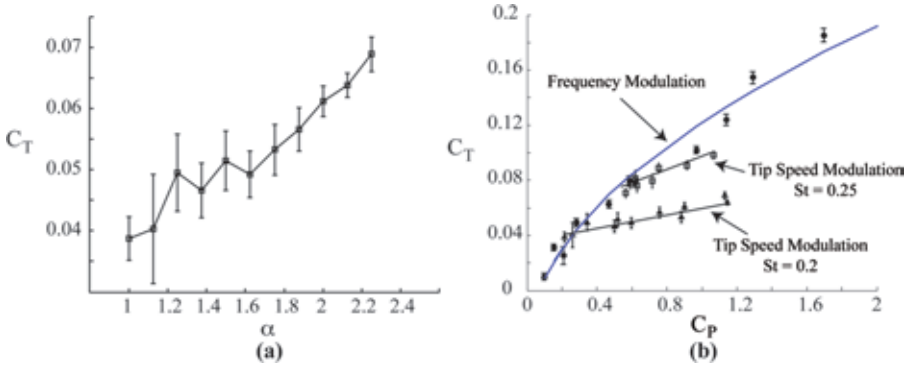

Figure 11 also reveals the role of passive flexibility. Here, the fin was actuated using only the two anterior spars, leaving the posterior half of the fin to respond passively to the forcing by the actuators and the fluid forces. The velocity of this fin still increases with increasing frequency, but the trend is no longer linear. Tests in still water indicate that the passive fin has a resonant frequency of about 2.4 Hz, defined as the frequency at which the trailing edge amplitude is maximized.

FIGURE 11

Fin velocity in chord lengths per second as a function of flapping frequency. The wavelength λ_a refers to the active fin while λ_p refers to the passive fin. (Color versions of figures available online at: http://www.ingentaconnect.com/content/mts/mtsj/2011/00000045/00000004.)

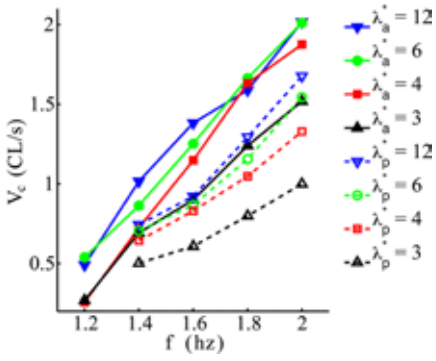

As resonance is approached, the amplitude of the trailing edge motion increases, resulting in the fin velocity increasing at an enhanced rate (in comparison to a linear trend). It should be noted that the swimming velocities for the passive fin were approximately 80% of those of the active fin.

The free-swimming Strouhal number for the active fin, along with manta ray field data (Fish, 2010), are displayed in Figure 12 (the Strouhal number for the passive fin is not shown since the trailing edge excursion of the passive fin is unknown). The experimental data collapse onto a single curve, indicating that the Strouhal number for the freely swimming active fin does not depend on the wavelength. As the swimming velocity increases, the Strouhal number begins to enter the regime presumed to be efficient (St = 0.2-0.4; Taylor et al., 2003). Hence, the optimal swimming speed for the traveling wave fin, from the perspective of efficiency, is likely to be ≥2 CL/s. The biological and experimental data display the same trend, whereby an increase in swimming velocity yields a decrease in Strouhal number. Borazjani and Sotiropoulos (2008, 2009) were able to show, for carangiform and anguiliform swimming, that the Strouhal number for self-propulsion approaches the efficient regime observed in nature only with increasing swimming velocity. The current study supports this conclusion for mobuliform swimming as well.

FIGURE 12

Strouhal number as a function of steady-state swimming velocity for the active fin compared with biological data of the manta ray (Fish, 2010).

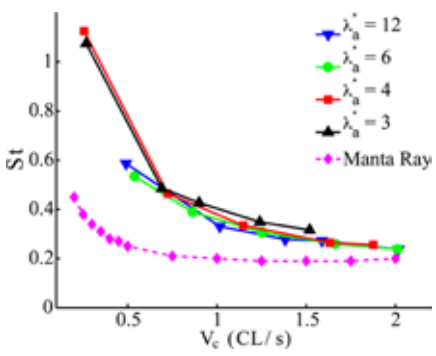

The energy economy, $\zeta = V_c/P_f$, for the active and passive fins is shown in Figure 13. In the case of the shortest wavelength($\lambda^* = 3$), the active fin has a higher energy economy than the passive fin, but for the longer wavelengths the energy economy for the passive fin

FIGURE 13

Energy economy as a function of flapping frequency. The wavelength λ_a refers to the active fin while λ_p refers to the passive fin.

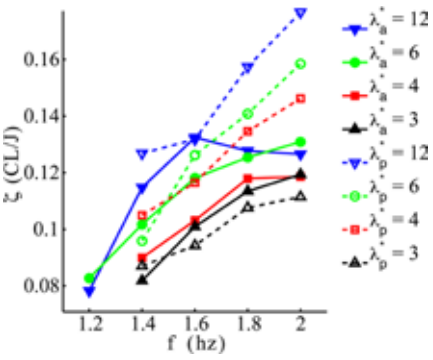

exceeds that of the active fin despite a decrease in the overall swimming speed (Figure 11). Clearly, by removing the two trailing edge spars in creating the passive fin, the power consumption decreases significantly compared to the active fin. The highest energy economy recorded was 0.18 CL/J for the passive fin with $\lambda_p^* = 12$ and f = 2 Hz, but its economy is still trending upward with increasing frequency, which may reflect the fact that the maximum test frequency was still below the resonant frequency of the fin (2.4 Hz). Leftwich and Smits (2010) found thrust production of a passively flexible artificial lamprey tail to increase as resonance is approached. The current work suggests that the energy economy also benefits by a system exploiting the resonant modes of a fin.

The increase in energy economy with frequency may also be a Strouhal number effect. Figure 12 indicates that the fin begins to enter the "efficient" regime (St = 0.2-0.4) with increasing swimming velocity (which occurs at higher flapping frequencies; see Figure 11). While the energy economy is not a direct measure of efficiency, the two parameters are inherently linked, so it is not altogether surprising that the energy economy increases as the Strouhal number approaches the supposedly optimal range. The active fin with $\lambda_a^* = 12$ displays a maximum at f = 1.6 Hz. It is believed that this peak is related to changes in the wake structure that result from the three-dimensionality of the wake associated with this fin. Dewey et al. (2011) found that an increasing wavelength causes the wake to bifurcate into a double wake structure that is less efficient, and it is believed to be responsible for the maximum observed in Figure 13. It may be that the other cases will eventually reach a maximum due to a similar mechanism, but further testing is required to support this suggestion.

Conclusions

This study has explored various kinematic modes associated with biological propulsion based on the manta ray. The results highlight the interdependence of the kinematic motions and fluid–structure interactions on the performance characteristics of the animal.

A purely heaving fin was used to examine three kinematic modes of swimming (flat, curved, and tip lag) as well as variation in the actuation waveform (sine waveform to square waveform). It was found that the flat mode of swimming produces higher efficiency and thrust compared to the curved mode of swimming. Furthermore, there was no performance benefit found by incorporating tip lag into the motion or by modulating tip speed instead of frequency. These results are counter to the hypothesis that as the motion becomes more biologically similar the thrust or efficiency performance will increase. The maximum thrust coefficient was found to be about 0.7 at St = 0.45, and the maximum propulsive efficiency was about 22% at St = 0.15. These performance metrics were low, as expected, due to the absence of a chordwise traveling wave motion. What was not expected was that the performance would be insensitive to curvature, tip lag, and tip speed variations. Without flexibility, the motion of the fin may be too constrained and not "natural" enough to achieve the performance benefits of the kinematic variations explored.

The presence of a chordwise traveling wave to generate an undulatory motion appears to be of prime importance for efficient propulsion. For example, Clark and Smits (2006) found efficiencies upwards of 50%. In free-swimming experiments of artificial fins similar to that studied by Clark and Smits, we found that they were able to generate speeds similar to those observed in nature, of the order 2 CL/s. When the fin was actively actuated, that is to say that the traveling wave motion was defined for all points on the chord of the fin, the steady-state Strouhal number obtained by the oscillating fin was found to be independent of the wavelength and exhibited the same trend as the manta ray in nature. That is, at low swimming velocities, both the manta ray and the artificial fin display high steady-state Strouhal numbers, but the Strouhal numbers decrease with increasing swimming speed and they approach the regime where efficient propulsion is hypothesized to exist (St = 0.2-0.4). Introducing passive flexibility into the fin, by restricting the actuation to the leading edge and letting the rest of the fin respond passively to the actuation and the external fluid forces, improved the energy economy. It was found that the passively actuated fin achieved steady state swimming speeds that were approximately 80% of that of the actively actuated fin, but because there was a significant decrease in the power required to propel the passively actuated fin the energy economy increased.

Acknowledgments

The authors would like to thank Daphne Rein-Weston, Dan Quinn, and Dr. Melissa Green for their aid in developing the low-friction carriage experiment. We would also like to thank Professor Frank Fish for correspondence regarding manta rays in nature. The authors would like to acknowledge funding from the Office

of Naval Research through the MURI program on Biologically-Inspired Autonomous Sea Vehicles (grant N0001408-1-0642), the David and Lucille Packard Foundation, the National Science Foundation (grant CMS-0384884), and the Virginia Space Grant Consortium.

Corresponding Author:

Alexander J. Smits
Mechanical and Aerospace Engineering, Princeton University
Princeton, NJ 08544
Email: asmits@princeton.edu

References

Anderson, J.M., Streitlien, K., Barrett, D.S., & Triantafyllou, M.S. 1998. Oscillating foils of high propulsive efficiency. J Fluid Mech. 360:41-72. doi: 10.1017/S0022112097008392.

Bandyopadhyay, P.R. 2005. Trends in biorobotic autonomous undersea vehicles. IEEE J Oceanic Eng. 30(1):109-39. doi: 10.1109/JOE.2005.843748.

Borazjani, I., & Sotiropoulos, F. 2008. Numerical investigation of the hydrodynamics of carangiform swimming in the transitional and inertial flow regimes. J Exp Biol. 211:1541-58. doi: 10.1242/jeb.015644.

Borazjani, I., & Sotiropoulos, F. 2009. Numerical investigation of the hydrodynamics of anguilliform swimming in the transitional and inertial flow regimes. J Exp Biol. 212:576-92. doi: 10.1242/jeb.025007.

Buchholz, J.H.J., & Smits, A.J. 2008. The wake structure and thrust performance of a rigid low-aspect-ratio pitching panel. J Fluid Mech. 603:331-65. doi: 10.1017/S0022112008000906.

Clark, R.P., & Smits, A.J. 2006. Thrust production and wake structure of a batoid-inspired oscillating fin. J Fluid Mech. 562:415-29. doi: 10.1017/S0022112006001297.

Colgate, J.E., & Lynch, K.M. 2004. Mechanics and control of swimming: A review. IEEE J Oceanic Eng. 29(3):660-73. doi: 10.1109/JOE.2004.833208.

Dewey, P.A., Carriou, A., & Smits, A.J. 2011. On the relationship between efficiency and wake structures of a batoid-inspired oscillating fin. J Fluid Mech. Under review.

Dong, H., Mittal, R., & Najjar, F.M. 2006. Wake topology and hydrodynamic performance of low-aspect-raio flapping foils. J Fluid Mech. 566:309-43. doi: 10.1017/S002211200600190X.

Fish, F.E. 2010. Private Communication.

Fish, F.E., Fegely, J.F., & Xanthopoulos, C.J. 1991. Burst-and-coast swimming in schooling fish (*Notemigonus crysoleucas*) with implications for energy economy. Comp Biochem Phys A Phys. 100:633-7. doi: 10.1016/0300-9629(91)90382-M.

Fish, F.E., Haj-Hariri, H., Smits, A.J., Bart-Smith, H., & Iwasaki, T. 2011. Biomimetic swimmer inspired by the manta ray. In: Biomimetics: Nature-Based Innovation, ed. Bar-Cohen, Y., 495-523. Boca Raton, FL: CRC Press.

Fish, F.E., Lauder, G.V., Mittal, R., Techet, A.H., Triantafyllou, M.S., Walker, J.A., & Webb, P.W. 2003. Conceptual design for the construction of a biorobotic AUV based on biological hydrodynamics. In: Proceedings of the 13th International Symposium on Unmanned Untethered Submersible Technology. Durham, NH: Autonomous Systems Undersea Institute.

Heathcote, S., & Gursul, I. 2007. Jet switching phenomenon for a periodically plunging airfoil. Phys Fluids. 19(2):027104. doi: 10.1063/1.2565347.

Heathcote, S., Wang, Z., & Gursul, I. 2006a. Effect of spanwise flexibility on flapping wing propulsion. In: 36th AIAA Fluid Dynamics Conference and Exhibit. Reston, VA: American Institute of Aeronautics and Astronautics Inc.

Heathcote, S., Wang, Z., & Gursul, I. 2006b. Flexible flapping airfoil propulsion at low Reynolds numbers. AIAA J. 45(5): 1066-79. doi: 10.2514/1.25431.

Heine, C. 1992. Mechanics of flapping fin locomotion in the cownose ray, *Rhinoptera bonasus* (Elasmobranchii, Myliobatidae). Ph.D. Thesis Duke University.

Jones, K.D., Dohring, C.M., & Platzer, M.F. 1998. Experimental and computational investigation of the KnollerBetz effect. Zool Anz. 173:1240-6.

Klausewitz, W. 1964. Der lokomotionsmodus der Flugelrochen (Myliobatoidei). AIAA J. 37:1240-6.

Leftwich, M.C., & Smits, A.J. 2010. Thrust production by a mechanical swimming lamprey. Exp Fluids. 50(5):1349-55. doi 10.1007/s00348-010-0994-x.

Liao, J.C. 2004. Neuromuscular control of trout swimming in a vortex street: Implications for energy economy during the Karman gait. J Exp Biol. 207:3495-506. doi: 10.1242/jeb.01125.

Liao, J.C., Beal, D.N., Lauder, G.V., & Triantafyllou, M.S. 2003. Fish exploiting vortices decrease muscle activity. Science. 302:1566-9. doi: 10.1126/science.1088295.

Rosenberger, L.J. 2001. Pectoral fin locomotion in batoid fishes: Undulation versus oscillation. J Exp Biol. 204(2):379-94.

Schmidt-Nielsen, K. 1972. Locomotion: Energy cost of swimming, flying, and running. Science. 177:222-8. doi: 10.1126/science.177.4045.222.

Taylor, G.K., Nudds, R.L., & Thomas, A.L.R. 2003. Flying and swimming animals cruise at a Strouhal number tuned for high power efficiency. Nature. 425(6959):707-11. doi: 10.1038/nature02000.